Computational models for dense snow avalanche motion

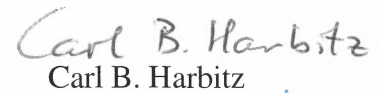581250-3   30 April 1996

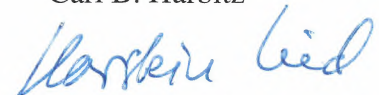**For the Norwegian Geotechnical Institute**

Project Manager:

Karstein Lied

Report prepared by:

Carl B. Harbitz

Reviewed by:

Karstein Lied

Computational models for dense snow avalanche motion

Report No: 581250-3
Date: 1996-04-30
Rev:
Rev. date:
Page: 2

NGI

Foreword

The present report is a contribution both to the joint avalanche research project «Norway-Iceland» supported by the Nordic Council of Ministers, and to the EU-program «Human Capital and Mobility», where the Norwegian effort is supported by the Norwegian Research Council (NFR).

NGI is thankful for the support that made it possible to accomplish the study.

Summary

Seventeen various models of dense snow avalanche motion are presented. These include statistical, comparative and energy considering models for run-out distance computations as well as dynamic models for avalanche motion simulations.

The latter describe either the internal dynamics of the material at certain stages of the motion, the dynamics of the moving mass as a whole from initiation to rest, or combinations of these. The dynamic models are presented with regard to the physical description of the moving material and to the mathematical and numerical modelling. Most of the dynamic models are rooted in hydraulic theory where the moving masses are described as a fluid, but also granular flow models inheriting geotechnical aspects of soil mechanics are included. Simple (quasi) three-dimensional models exist, but most of the models are still of one and two dimensions.

Rather than expanding more existing models into three dimensions, the author suggests to improve the one- and two-dimensional dynamic models further, preferably by combining models based on Bagnold's (1954) concept of dispersive pressure and dynamic shear with granular flow models involving aspects of soil mechanics. Density variations, nonhomogeneous concentration, particle size distribution, cohesion, particle rotation as well as temperature changes and energy dissipation are not adequately described in any of the dynamic models. Furthermore there is a conspicuous lack of any description of stability and accuracy of the applied numerical methods.

Examples of travel distance computations based on one statistical, one comparative and three dynamic models are finally presented for four Norwegian avalanches.

Computational models for dense snow avalanche motion

Report No: 581250-3
Date: 1996-04-30
Rev:
Rev. date:
Page: 4

NGI

Contents

Review and reference document

Computational models for dense snow avalanche motion

Report No: 581250-3
Date: 1996-04-30
Rev:
Rev. date:
Page: 5

1   INTRODUCTION

The scope of the present report is to give a survey of the various kinds of computational models for calculating dense snow avalanche motion and run-out.

Most avalanches consist of at least two parts. One is referred to as a dense snow avalanche (or flowing avalanche, in this report simply referred to as avalanche), which is a gravity flow. The other is a turbidity part referred to as an (airborne) powder avalanche, which is driven by the extra weight of small snow particles (< 1 mm) suspended in the air. A fully developed avalanche can be divided in four flow layers (Norem 1995a). The major volume of the avalanche is represented by the basal and liquefied *dense flow layer*, where the particles are in close contact, and the volumetric density is high. The density is assumed to be almost constant. Above the dense flow layer is the transitional *saltation layer,* where the particles are transported in jumps similar to saltating particles in drifting snow. The volumetric density is reduced to the power of three with height in the saltating layer. Then follows the *suspension layer* that constitutes the snow cloud of the avalanche. Here the density and the velocity are both reduced almost linearly with height. Above and around the avalanche is a backflow of air named the *recirculation layer*, with a height one to three times that of the suspension layer.

Since the material properties differ, the distinction between wet snow (generally cohesive with possible snowball formation) and dry snow (no free water content) avalanches is useful. Dense snow avalanches can occur under both wet and dry snow conditions. A turbidity part is normally generated in both circumstances, especially in steep slopes. Pure powder avalanches require dry snow conditions.

Both wet snow and dry snow avalanches involve high internal deformation and are more or less in a liquid state. For wet snow avalanches, solid concentrations are high (inertial regime), and energy dissipation is caused mainly by particle interactions. In dry snow avalanches, energy dissipation is caused mainly by particle interactions at high solid concentrations, and by viscosity in the interstitial air at low concentrations (macro-viscous regime). Both flow regimes give rise to a dynamic shear and to a dispersive stress normal to the flow direction reducing internal friction, as described by Bagnold (1954, 1956).

The type of rupture of the snow cover depends on the state of intergranular cohesion. In loose snow a point fracture occurs (a loose snow avalanche), whereas sufficient intergranular cohesion favours line fracture and the resulting avalanche moves initially as a slab before it breaks down.

The first attempt to formulate a general theory of avalanche motion was made

Computational models for dense snow avalanche motion

Report No: 581250-3
Date: 1996-04-30
Rev:
Rev. date:
Page: 6

NGI

by Voellmy (1955), and this theory is still widely used. Increased human activity in mountain regions, deforestation from pollution, forestry and ski resorts as well as anticipated warming of the earth's atmosphere have caused a growing interest in the study of catastrophic avalanches. Both statistical, comparative and energy considering models for run-out distance computations as well as dynamic models for avalanche motion simulations are now developed. However, no universal model has so far been made. The dynamics of avalanches are complex, involving both fluid, particle and soil mechanics. The limited amount of data available from real events makes it hard to evaluate or calibrate existing models. Often several models with different physical descriptions of the avalanche movement can all fulfil the deficient recorded observations.

The dynamic models included in the present report are discussed in terms of the physical description of the dynamics, and the material properties of the flowing snow. Assumptions and simplifications inherent in the mathematical equations of each model are outlined, as well as possible numerical methods and results. The limitations and practical applications of each model are discussed. All models in common use are one- or (quasi) two-dimensional. One three-dimensional model is presented (Lang and Leo, 1994), although it is still unknown if it represents naturally occurring events.

Dynamic models of avalanches can be divided into two groups:
• The sliding block model describes the avalanche as a rigid block on an inclined plane. This model describes well the slide initiation. Due to its simplicity it is also widely used for the continuation. Only the translation of the mass centre is described. Back-calculated friction coefficients tend to be low compared with measured values.
• Deformable body models describe the sliding mass as a continuum. Difficulties arise in choosing convenient constitutive equations, boundary conditions, initial conditions and in solving the equations.

To limit the extent of the report, models exclusively developed for powder snow avalanches are not included. As opposed to dense snow avalanches, this airborne turbulent particle flow is rather described by density current models or binary (solid-fluid) mixture models (cf. Savage and Hutter, 1990). For a review, see Brørs (1991), Hermann and Hutter (1991) and Tesche (1986).

Also papers on material properties or physical experiments of dense snow avalanches, release mechanisms, impact pressure, defence structures, descriptions of case studies or other related topics are omitted when not including any aspects of dynamic modelling or run-out distance calculations. For further studies, the following review papers are referred: Hopfinger (1983), Hutter (1991), Mellor (1978), Norem (1992a, 1995b), Perla (1980) and Scheiwiller and Hutter (1982).

Computational models for dense snow avalanche motion

Report No: 581250-3
Date: 1996-04-30
Rev:
Rev. date:
Page: 7

NGI

With other parameter values or minor modifications, many of the models originally designed for other kinds of slide motion (rock slides, debris flows, etc.) should also be applicable for avalanches. A survey of computational models for rock slide and debris flow motion is given by Harbitz (1996).

As part of the joint avalanche research project between Norway and Iceland, new avalanche models are developed in Iceland at the time being. These models will be described later in a certain report by the avalanche researchers connected to Veðurstofa Íslands (Icelandic Meteorological Office).

2   THE LIED AND BAKKEHØI STATISTICAL α/β-MODEL

The statistical α/β-model (Lied and Bakkehøi, 1980, Bakkehøi et al., 1983, Lied and Toppe, 1988, Bakkehøi and Norem, 1994) was developed at NGI and governs maximum run-out distance solely as a function of topography. The run-out distance equations are found by regression analysis, correlating the longest registered run-out distance from 206 avalanche paths to a selection of topographic parameters. The parameters that have proved to be most significant are presented in Table 2.1, cf. Fig. 2.1:

Table 2.1   Topographic parameters governing maximum run-out distance.

Symbol of parameter:	Parameter description:
β (deg.)	Average inclination of avalanche path between starting point and point of 10° inclination along terrain profile.
θ (deg.)	Inclination of top 100 vertical meters of starting zone.
H (m)	Total height difference between starting point and lowest point of best fit parabola $y=ax^2+bx+c$.
y'' (m^{-1})	Curvature of avalanche path.

The β-angle is empirically found to be the best characterisation of the track inclination.

The inclination θ of the top 100 vertical metres of starting zone indirectly governs the rupture height, and thereby the slide thickness, which is greater in gentle slopes than in steep slopes. Hence smaller values of θ give longer run-out distances or smaller average inclination of the total avalanche path, α.
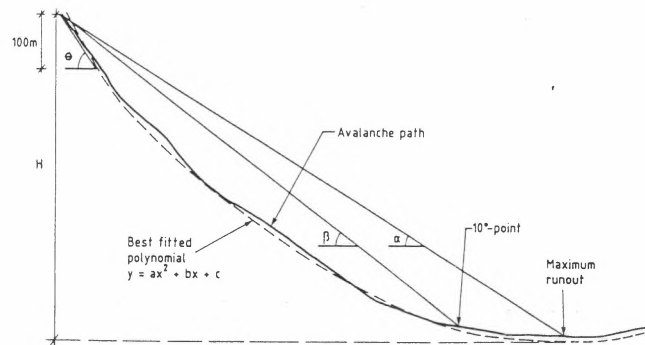
Computational models for dense snow avalanche motion

Report No: 581250-3
Date: 1996-04-30
Rev:
Rev. date:
Page: 8

NGI

Fig. 2.1   Topographic parameters describing terrain profile (after Lied and Toppe, 1988).

In Norway most avalanche paths might be approximately described by the parabola $y=ax^2+bx+c$, of which curvature is described by the second derivative $y''=2a$.

In slide paths with little difference in height, H, a smaller part of the potential energy is transformed into heat by friction. Hence the avalanches have an apparently lower coefficient of friction, and obtain theoretically a smaller run-out angle.

For a parabolic slope, the β-angle is determined by $\beta = \tan^{-1}\left(\sqrt{\dfrac{Hy''}{2}} + \dfrac{\tan 10°}{2} \right)$.

Smaller values of the product Hy'' mean smaller values of β. This results in smaller values of α, because the avalanches run with smaller velocity, and the velocity-dependent frictional transformation of potential energy into heat is reduced.

The topography, the width and the degree of lateral confinement in the starting zone, as well as the drifting snow transport into the starting zone, have little influence upon the run-out distance (Lied and Bakkehøi, 1980, Lied et al., 1995). As opposed to what was presumed, no tendency was found that an avalanche with a wide rupture zone, which is channelled into a narrow track, has a longer reach than an avalanche following an unconfined path.

The regression analysis revealed that the β-angle is the most important topographic parameter. The result of the regression analyses is referred in Table 2.2.

Computational models for dense snow avalanche motion

Report No: 581250-3
Date: 1996-04-30
Rev:
Rev. date:
Page: 9

Table 2.2   *Results of regression analysis (translated from Bakkehøi and Norem, 1994) with standard deviations (SD) and correlation coefficients (R). [H] represents the numerical value of H.*

Assumption	No. of avalanches	Regression equation, $\alpha=$	Accuracy		Standard deviation (m) H=1000m, horizontal run-out		
			SD (deg.)	R [-]	α (deg.)	$-\Delta L$ (m)	ΔL (m)
$\beta \leq 30°$	68	$0.89\beta + 0.035\theta - 2.2° \cdot 10^{-4}[H] - 0.9°$	1.49	0.84	25	138	154
$30° < \beta \leq 35°$	59	$1.15\beta - 2.5° \cdot 10^{-3}[H] - 5.9°$	2.50	0.53	30	162	189
$\beta > 35°$	79	$0.81\beta + 0.036Hy''\theta + 3.2°$	2.67	0.62	36	127	144
$\beta \leq 30°,$ $H \geq 900m$		$0.94\beta + 0.035\theta - 2.6°$	1.02	0.90	25	96	103
All avalanches	206	$0.96\beta - 1.4°$	2.30	0.92			
All avalanches	206	$0.92\beta - 7.9° \cdot 10^{-4}[H] + 0.024Hy''\theta + 0.04°$	2.28	0.92			

The model is most appropriate for travel distance analysis along longitudinally concave profiles. The calculated run-out distances are those that might be expected under snow conditions favouring the longest run-out distances. The authors have no explanation as to why there is such a small correlation in the data for $30° < \beta \leq 35°$.

Lied and Toppe (1988) redefine the starting zone as the part of the path lying between the starting point and the point of $30°$ inclination along the terrain profile. The average inclination of this zone is termed γ. They further describe the automatic computation of the avalanche parameters. Applying the relation $\alpha = f(\beta, \gamma)$ for 113 avalanches, the equation $\alpha = 0.91\beta + 0.08\gamma - 3.5°$ gives $R^2 = 0.94$ and SD=1.4°, which is a small improvement to the relation between α and β in Table 2.2. Lied and Toppe (1988) also present combinations of the lengths of the starting zone, the avalanche track and the run-out zone, L_1, L_2 and L_3 respectively as well as the area A of the starting zone (evaluated subjectively from local topography as a substitute for the avalanche volume). The best relation is $L \equiv L_1 + L_2 + L_3 = 0.93L_1 + 0.97L_2 + 0.61m \cdot [A] + 182m$, with $R^2 = 0.96$ and SD=137m ([A] represents the numerical value of A [m^2]). Using L_3 alone as the dependent variable does not give R- and SD-values that enable sufficiently accurate calculations of run-out distance. The prediction of path lengths will give run-out distances independent of steepness of path, as opposed to the more realistic α/β-relations. McClung and Lied (1987) show that the avalanches with the 50 highest values of the ratio $L_3/(L_1 + L_2)$ give a very good fit to an extreme value distribution.

The assumption of small variations in the physical snow parameters giving the longest run-out distance is only valid within one climatic region (McClung et

048. Bra-Trykk AS

Computational models for dense snow avalanche motion

Report No: 581250-3
Date: 1996-04-30
Rev:
Rev. date:
Page: 10

al., 1989). Martinelli (1986) and McClung et al. (1989) have applied the basics of the statistical α/β-model in mountain regions outside Norway.

The avalanche database of NGI is constantly extended, and contains at present 230 events. Both the statistical and the dynamic models are occasionally recalibrated.

Examples of run-out distance computations based on the α/β-model are presented in sec. 19.

3 THE BAKKEHØI COMPARATIVE MODEL

Buser (1983) and Buser et al. (1987) developed a method to evaluate the similarity between two meteorological situations. Thus they were able to compose an avalanche hazard warning for the actual day by finding the earlier days with the most similar conditions, and studying the registered avalanche activity on those days.

Bakkehøi and Norem (1993, 1994) use the same method to estimate avalanche run-out angle α (average gradient of the avalanche path) along a certain path profile. The actual profile is compared with registered path profiles of more than 200 previous avalanche events. The average inclination of the avalanche path between starting point and point of 10° inclination along terrain profile, β, is considered the most important parameter governing the run-out angle. Thus avalanche path profiles in the register with β-values differing more than two degrees from the actual profile, are excluded from the investigation. Each remaining avalanche path profile and its best fit parabola y(x) are described by the characteristic parameters presented in Table 3.1 (cf. the statistical α/β-model above). All parameters are weighted by suitable coefficients w_i.

When comparing the actual profile with a profile from the avalanche data register, the seven parameters in Table 3.1 will take different values for the two paths, x_{i1} and x_{i2}, i=1,2,...,7, respectively. The similarity between the two paths is expressed by the 7-dimensional weighted distance

$$d = \sqrt{\sum_{i=1}^{7} w_i (x_{i1} - x_{i2})^2}$$

where a small value of d indicates a high degree of similarity. The actual run-out angle is finally calculated as the average of the run-out angles of the five most similar registered avalanche path profiles.

Computational models for dense snow avalanche motion

Report No: 581250-3
Date: 1996-04-30
Rev:
Rev. date:
Page: 11

NGI

Table 3.1   Parameters describing avalanche path profile.

Symbol of parameter x_i:	Parameter description:	Weight coefficient w_i:
θ	Inclination of starting zone.	0.3
y''	Shape factor, $y''=2a$. Describes curvature of best fit parabola $y=ax^2+bx+c$.	0.3
H	Total height difference between starting point and lowest point of best fit parabola $y=ax^2+bx+c$.	0.04
z	Altitude of run-out area (m.a.s.l).	0.03
H y''	Determines β angle for a parabolic slope by $$\beta = \tan^{-1}\left(\sqrt{\frac{Hy''}{2}} + \frac{\tan 10°}{2} \right)$$	0.7
σ	Standard deviation of best fit parabola from the coordinates ot the given path profile.	1.0
Q	Standard deviation of variation of deviation of best fit parabola from the coordinates of the given path profile. Q expresses the roughness of the path profile.	2.0

Evaluation of the method is accomplished by Bakkehøi and Norem (1994). The standard deviation of the calculated run-out angle from the observed run-out angle for all the registered avalanches is 1.86°. This is better than the standard deviation for both the statistical α/β-model (sec. 2) and the NIS model (sec. 12), which is 2.2° and 2.3° for the whole avalanche register respectively.

The comparative model also gives the opportunity to study the background material of the most similar registered avalanche events with regard to topographical conditions, regional climate, and accuracy of return period. Hence it is possible to attach greater importance to selected registered events.

Examples of run-out distance computations based on the comparative model are presented in sec. 19.

4   THE KÖRNER ENERGY LINE BLOCK MODEL

The Körner (1980) energy line model describes a rigid body that slides along a path with constant coefficient of dry friction, f_r. The energy line results from the graphical representation of the law of conservation of energy, which states that the sum of potential energy plus kinetic energy plus energy losses that occur, is constant along the path. When the energy losses is due to dry friction only, the energy line corresponds to the straight line between the position of rest of the centres of gravity of the sliding mass before and after the movement, Fig. 4.1:
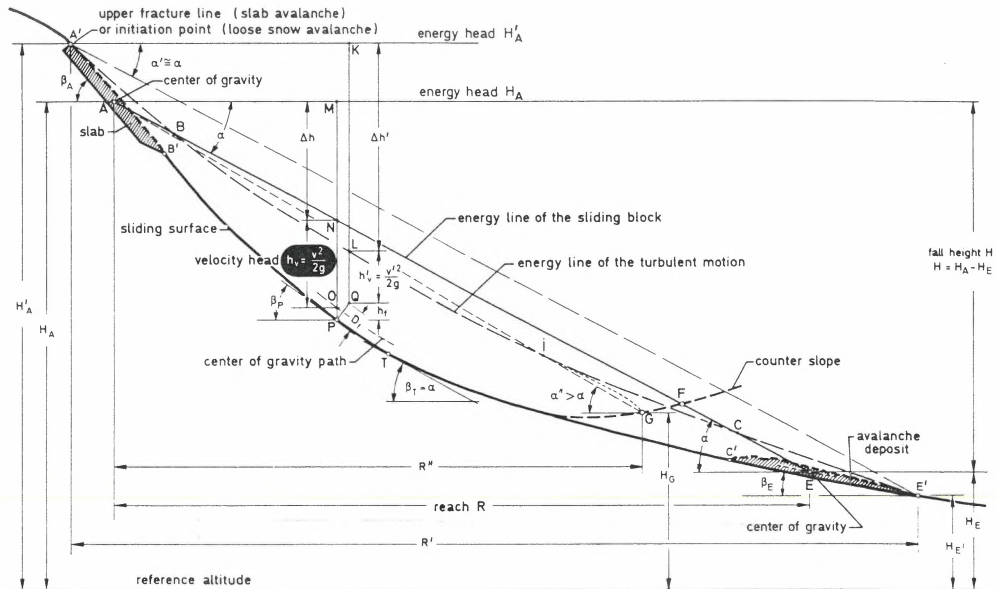
Computational models for dense snow avalanche motion

Report No: 581250-3
Date: 1996-04-30
Rev:
Rev. date:
Page: 12

NGI

Fig. 4.1:Avalanche-path profile with the energy lines (after Körner, 1980).

The slope angle of this line is given by

$$\tan \alpha = \frac{H}{R} = \frac{\text{fall height}}{\text{reach}} = f_r$$

Empirical values of α can be used to determine the reach by plotting the energy line from the starting point. The terminal point of the movement is always where the centre-of-gravity path A-E (or the slide path as an approximation) intersects the energy line.

The velocity v of the block for every point along the path is determined by

$$v = \sqrt{2gh_v}$$

where h_v is the distance between the path of the centre of gravity and the energy line, and g is the acceleration of gravity.

Körner (1976, 1980) also discusses how the energy line model can be applied to determine the two coefficients μ and ξ of the Voellmy model described below. An example of application is included.

Zenke and Hildebrandt (1983) extend the method to include a coefficient of friction varying along the path. The coefficient values at each path segment

Computational models for dense snow avalanche motion

Report No: 581250-3
Date: 1996-04-30
Rev:
Rev. date:
Page: 13

NGI

represent the regression coefficients and are multiplied by the relative length of each segment in a linear regression equation expressing the calculated overall friction coefficient. The coefficients are determined by minimising the difference between the calculated overall friction coefficient and the observed friction coefficient expressed by $\tan\alpha$. Calculated coefficients of friction are presented as functions of both avalanche cross-sections along the path and avalanche scar area.

5   THE VOELLMY BLOCK MODEL

Voellmy's (1955) model is a one-dimensional block model for the calculation of avalanche run-out distance.

The sliding mass is considered as an endless fluid of height H reaching a terminal velocity by equilibrium of gravitational forces and shear forces on an infinitely long slope of constant inclination θ_1. Based on hydraulic theory, the shear forces are represented by a dynamic drag proportional to the terminal velocity squared on the free, upper surface and a combination of a similar dynamic drag and a Coulomb friction proportional to the normal forces along the bed. Hence the terminal velocity is expressed by the two-parameter formula

$$V_t = \left[\xi\, H (\sin\theta_1 - \mu\cos\theta_1) \right]^{1/2}$$

where density and drag coefficients are lumped together into the «coefficient of turbulent friction», ξ [m/s^2], and μ is the Coulomb friction coefficient. To account for lateral confinement, H is replaced by the hydraulic radius (flow cross-sectional area divided by wetted perimeter).

The deceleration starts at a certain reference point, normally located where the actual slope inclination equals $\tan^{-1}\mu$. From this point the run-out distance on a slope of constant inclination θ_2 is computed by energy considerations:

$$S = V_t^2 \left[2g(\mu\cos\theta_2 - \sin\theta_2) + V_t^2 g / (\xi\, H_D) \right]^{-1}$$

H_D is the mean depositional depth accounting for the energy loss due to pile-up of debris and g is the acceleration of gravity.

The computed run-out distance is based on the assumption that terminal velocity is reached, and depends strongly on the selected location of the reference point, as well as on the values of the input parameters.

The values of μ and ξ are discussed by Buser and Frutiger (1980) and by Martinelli et al. (1980).

Computational models for dense snow avalanche motion

Report No: 581250-3
Date: 1996-04-30
Rev:
Rev. date:
Page: 14

NGI

6 THE PCM BLOCK MODEL

The 2-parameter PCM-model (Perla, Cheng and McClung, 1980) is a further development of Voellmy's model above. The avalanche is described as a one-dimensional block of finite mass moving on a path of varying curvature. The reference point is the initial rest position of the block's centre of mass. The equation of momentum includes Coulomb friction, centrifugal force due to curvature of the path, dynamic drag and inertia resistive ploughing. The Coulomb friction term consists of an adjustable friction coefficient μ multiplied by the normal force along the bed. The latter three terms are all proportional to v^2, the tangential velocity squared, and hence lumped together into one term consisting of v^2 divided by the second adjustable parameter interpreted as a mass-to-drag ratio, M/D [m^{-1}]. The result is a linear differential equation in v^2:

$$\frac{1}{2}\frac{dv^2}{ds} = g(\sin\theta - \mu\cos\theta) - \frac{D}{M}v^2$$

where θ is the local inclination, s is the slope position and g is the acceleration of gravity. However, the inclination and perhaps the adjustable parameters are not constant along the path. An iterative solution procedure is described, dividing the slope into small segments of constant inclination and parameter values. To compensate for the absence of curvature along the linear segments, the velocity is corrected for conservation of linear momentum at each segment transition.

The usefulness of the model depends on a knowledge of the two adjustable parameters that can vary considerably, cf. Table 19.1. For avalanches, these values have been limited to some extent by testing the model statistically on 136 extreme paths in Northwest USA and Norway (Bakkehøi et al., 1981) and on 206 extreme paths in Norway (Bakkehøi et al., 1983).

Alean (1984, 1985) has analysed nineteen ice avalanches to establish parameter values and test whether the PCM-model might be applicable for such events. He concludes that deviations between model predictions and observations are «disappointingly high», and that a one-parameter model leads to only slightly worse predictions of run-out distances for ice avalanches.

For constant inclination and parameter values along an infinitely long slope, the result is analogous to that of Voellmy.

7 THE NOHGUCHI MASS CENTRE PATH MODEL

The Nohguchi (1989) model is a three-dimensional model for mass centre motion of an avalanche on a surface of arbitrary configuration. The equations describing the motion are derived by classical mechanics (Goldstein, 1980),

Computational models for dense snow avalanche motion

Report No: 581250-3
Date: 1996-04-30
Rev:
Rev. date:
Page: 15

including the restriction force on the flowing mass from the ground, and a resistance force represented by dynamic drag and Coulomb friction (as in the Voellmy model). The point mass is constrained to the surface by requiring that the vertical component of the normal force from the ground is directed upwards.

The equations are solved numerically by the Runge-Kutta method. Numerical simulations of real avalanches are presented. For suitable choices of the parameter values of ξ, H and μ (determining the terminal velocity, cf. Voellmy's model) the avalanche follows the observed path. However, the simulated avalanche path is strongly dependent on the parameter values. The deviation from the steepest path through the curves increases with increasing terminal velocity.

Simulations of real travel paths can be used to determine appropriate parameter values.

8 THE VSG REFINED BLOCK MODEL

The VSG-model (Voellmy, 1955, Salm et al., 1990, Salm, 1993 and Gubler, 1993) is the most commonly used model for calculation of avalanche motion in Switzerland and Austria.

The model assumptions are incompressibility of flow along the whole path, steady flow and small variations of flow height along the track (i.e. between starting and run-out zones) and non-steady quasi-rigid body movement in the run-out zone. The model is quasi two-dimensional as it to some extent incorporates the average width of the starting zone, the track and the run-out zone separately, as well as the cross-sectional shape of the track.

The computed velocity v_0 of the mass centre leaving the starting zone is computed in correspondence with the terminal velocity of Voellmy's model (for avalanches a default value of initial flow height d_0 is presented based on statistical analysis of precipitation data from Swiss mountain areas). Given the width of the starting zone, W_0, the model computes the flow rate $Q = W_0 d_0 v_0$. The terminal velocity at the bottom of the track

$$v_p = \left[\frac{Q}{W_p} \xi \, (\sin \psi_p - \mu \cos \psi_p) \right]^{1/3}$$

is based on the average width W_p of a «control section» of a few hundred meters (theoretical length is suggested in Gubler (1993)) at the lower end of the track, μ and ξ are the same coefficients as in Voellmy's model, and ψ_p is

Computational models for dense snow avalanche motion

Report No: 581250-3
Date: 1996-04-30
Rev:
Rev. date:
Page: 16

NGI

inclination of control section. For laterally confined tracks the terminal velocity is given by

$$v_p = \left[R\xi \, (\sin \psi_p - \mu \cos \psi_p) \right]^{1/2}$$

where R is the hydraulic radius. Dynamic pressure on obstacles along the track is calculated.

The run-out zone is said to begin where the inclination equals $\tan^{-1}\mu$. (Thus the run-out zone starts on more gentle slopes for larger avalanches because the assumed μ values are smaller). By time-dependent modelling of the movement of the avalanche front, and assuming a linear decrease of the velocity squared

$$v^2 = d_s\xi \, (\mu \cos \psi_s - \sin \psi_s)$$

in the run-out zone of average inclination ψ_s, the length of the run-out zone is

$$s = \frac{d_s}{2g} \ln\left(1 + \frac{v_p^2}{v^2} \right)$$

where g is the acceleration of gravity and deposit height $d_s = \dfrac{Q}{W_p v_p} + \dfrac{v_p^2}{4\lambda g}$.

The internal friction parameter of the avalanche mass, λ, determines the transfer of kinetic energy (particle speed) to potential energy (flow height). According to Harbitz (1995), the model results are not very sensitive to the value of λ (equals 2.5 for wet, dense snow avalanches). The run-out zone might be divided into small segments for altering the parameter values and computing the velocity along the slope. The numerical program returns both the limit of the red zone (i.e. where the dynamic pressure exceeds 30 kPa) and the total run-out distance.

An alternative run-out model is also included (Salm, 1993), applicable when there is no enlargement of the flow width in the run-out zone. Now the flow is modelled as a flexible sliding sheet with high internal friction. The model results in lower (more realistic) deposit heights and a faster decrease of flow speed in the run-out zone. This run-out model is more dependent on the value of the internal friction parameter (Harbitz, 1995).

The results of the VSG-model are critically dependent on the input values of width, length and inclination of the starting zone, initial flow height h_0, friction coefficients, cross-section of the track and inclination of the track and the run-out zones, cf. Table 19.1. A default value of the initial flow height is presented according to the Swiss guidelines (Salm et al., 1993), based upon the altitude of the fracture line, the return period of the avalanche and the climatic region.

Computational models for dense snow avalanche motion

Report No: 581250-3
Date: 1996-04-30
Rev:
Rev. date:
Page: 17

NGI

The model has been tested for avalanches by Buser and Frutiger (1980), Föhn and Meister (1982), Gubler (1987) and Lied et al. (1995). The latter concluded that the uncertainties for the VSG-model are as great as for the PCM- and NIS-models.

9 THE HUNGR MULTI-MATERIAL DEFORMABLE BODY MODEL

Hungr (1995) has developed a deformable body model for simulating the characteristics of non-steady rapid flowslides, debris flows and avalanches. The model is quasi two-dimensional based on vertically integrated equations of balance of mass and linear momentum and with a simplified lateral confinement. The slide mass is represented by a number of blocks contacting each other, free to deform and retaining fixed volumes of material along a vertically curved path.

The block representation leads to a Lagrangian centred finite difference explicit numerical solution referenced to curvilinear coordinates and a moving mesh. The momentum equation is applied to narrow columns of the flow, called «boundary blocks». The continuity equation for balance of mass is applied to «mass blocks» of fixed volume separating the boundary blocks. All interpolations are predicated on the assumption that both flow surface and path are reasonably smooth. Smoothness of the path profile is ensured by spline function fitting.

The driving force, F, acting on each boundary block of heights H_i and widths B_i, i=1 to n, consists of the tangential component of weight, the basal resisting force, T (described below), and the tangential internal pressure resultant:

$$F = \gamma \ H_i B_i ds \ \sin \alpha + P - T$$

where γ is the bulk unit weight and α is the inclination (the nominal length ds of the boundary block, measured in the direction of the curvilinear coordinates, cancels out in the equations, once all the forces are evaluated).

The new velocity, v_i, of each boundary block at the end of a time step is obtained from the old velocity, v_i', by numerical integration of Newton's second law:

$$v_i = v_i' + \frac{g(F\Delta t - M)}{\gamma \ H_i B_i ds}$$

where Δt is the time increment, and g is the acceleration of gravity. The term M is a momentum flux resulting from material deposition (M=0) or entrainment (M=$\Delta m \cdot v$, where Δm is the mass increment entrained during the time step).

Computational models for dense snow avalanche motion

Report No: 581250-3
Date: 1996-04-30
Rev:
Rev. date:
Page: 18

NGI

The erosion or deposition rates of each boundary and mass block are assumed constant percentages of the cross-sectional area per unit displacement. The volume changes are applied only in designated zones along the path.

A second integration is used to obtain the curvilinear displacements, S_i, of the boundary blocks following the time step (old displacements primed):

$$S_i = S_i' + \frac{\Delta t}{2}(v_i + v_i')$$

The new positions of the boundary blocks are now known. The average depth of the flow in the mass blocks, h_j, j=1 to n-1, is determined so as to maintain their constant volume, V_j:

$$h_j = \frac{V_j}{(S_{i+1} - S_i)(B_{i+1} + B_i)/2}$$

The new height of each boundary block is calculated as the mean of the depths of the adjacent mass blocks:

$$H_i = \frac{h_{j-1} + h_j}{2}$$

while the end mass blocks are assumed to be triangular:

$$H_1 = \frac{h_1}{2} \qquad\qquad H_n = \frac{h_{n-1}}{2}$$

A lateral pressure coefficient k reflects the longitudinal rigidity of the flowing mass. It depends on the tangential compressive strain, and is defined both for the boundary blocks, k_i, and for the mass blocks, k_j. Under hydrostatic conditions k equals 1, and for a dry granular material with friction, it may range between the active and passive coefficients k_a and k_p. The longitudinal pressure gradient at each boundary block is obtained as the average for the two adjacent mass blocks using the following equation (s_j values are the curvilinear displacements of the mass block centres):

$$k_i \frac{dH}{ds} = \frac{1}{2}\left[\frac{k_j(h_j - H_i)}{s_j - S_i} + \frac{k_{j-1}(H_i - h_{j-1})}{S_i - s_{j-1}}\right]$$

The coefficient k_j is increased or decreased by a value equal to the incremental strain times a stiffness coefficient, as shown in Fig. 9.1:

$$k_j = k_j' + S_{cu}\Delta\varepsilon_j$$

Computational models for dense snow avalanche motion

Report No: 581250-3
Date: 1996-04-30
Rev:
Rev. date:
Page: 19

NGI

where the stiffness coefficient S_{cu} is taken as $S_c = (k_p - k_a)/0.05$ for compression and $S_u = (k_p - k_a)/0.025$ for unloading. The minimum and maximum values that k_j can reach correspond to the active and passive states. The incremental strain in each mass block during a time step, $\Delta\varepsilon_j$, is calculated from the displacements of the adjacent boundary blocks:

$$\Delta\varepsilon_j = \frac{(S_{i+1} - S_i) - (S'_{i+1} - S'_i)}{S'_{i+1} - S'}$$

Now the longitudinal pressure differential on each boundary block may be determined as:

$$P = k\gamma \frac{dH}{ds}\left(1 + \frac{a_c}{g}\right)H_i B_i \cos\alpha \; ds$$

based on the assumption that the flow lines are approximately parallel with the bed and that the pressure parallel with the path increases linearly with depth. $a_c = v_i^2/R$ is the centrifugal acceleration, dependent on the vertical curvature radius of the path, R.

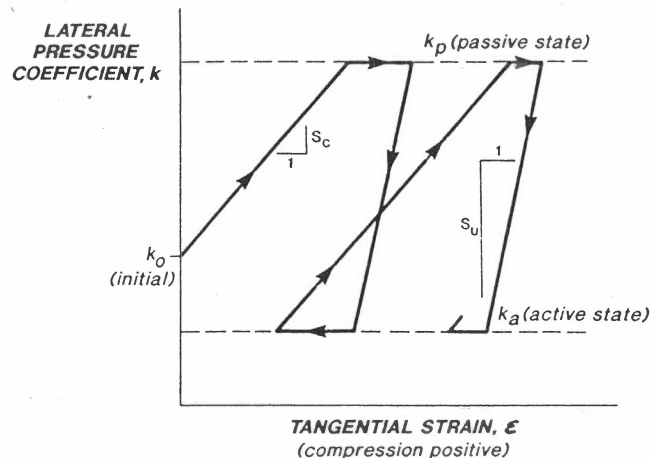*Fig. 9.1:* *Method of calculating the lateral pressure coefficient k in a mass element as a function of changing tangential strain. Initially, k is equal to an «at rest» coefficient k_0, usually 1.0. As each mass block expands or contracts during motion to maintain geometric compatibility, k changes following a path similar to that shown in the diagram. Stiffness coefficient: S_c, compression; S_u, unloading (after Hungr, 1995).*

Computational models for dense snow avalanche motion

Report No:	581250-3
Date:	1996-04-30
Rev:	
Rev. date:	
Page:	20

NGI

The functional relationship between T and other parameters of the flow is based on the assumption that the shear stress on tangential planes increases linearly with normal depth. This, together with a given rheological constitutive equation, determines a velocity-depth distribution profile and an equation for T. The model allows the selection of seven material rheological functions (the boundary block base $A_i = ds\ B_i$):

1. *Plastic flow*: This flow is controlled by a constant shear strength, such as the steady state undrained strength, c, of liquefied material:

$$T = cA_i$$

2. *Friction flow*: T is a function only of the effective normal stress on the base of the flow. This stress depends on flow depth, bulk unit weight and pore pressure:

$$T = A_i \gamma\ H_i \left(\cos\alpha + \frac{a_c}{g} \right)(1 - r_u)\tan\phi$$

where r_u is the pore pressure coefficient (ratio of pore pressure to the total normal stress at the base of the block) which might be a function of location or elapsed time (drainage). The friction angle, ϕ, can be a function of displacement to simulate the decay of strength from peak to residual.

3. *Newtonian laminar flow*: T is a linear function of velocity with a dynamic viscosity μ. The flow resistance term is determined by the Poiseuille equation:

$$T = \frac{3A_i v_i \mu}{H_i}$$

4. *Turbulent flow*: T is a function of velocity squared. For water flow, the Manning equation with the roughness coefficient n can be used:

$$T = A_i \gamma\ v_i^2 n^2 H^{-\frac{1}{3}}$$

5. *Bingham flow*: The resisting force is a function of flow depth, velocity, constant yield strength, τ, and Bingham viscosity, μ. As for the Newtonian laminar flow, the mean flow velocity is derived from an assumption of a linear increase of shear stress with depth:

$$v_i = \frac{H_i}{6\mu}\left(\frac{2T}{A_i} - 3\tau + \frac{\tau^3 A_i^2}{T^2} \right)$$

The determination of T requires a solution of the cubic equation above. The

048. Bra-Trykk AS

Computational models for dense snow avalanche motion

Report No: 581250-3
Date: 1996-04-30
Rev:
Rev. date:
Page: 21

velocity profile associated with this formulation contains a rigid plug, riding on a zone of distributed shear. The thickness of the plug equals $\tau\, H_i\, /\, T$.

6. *Coulomb viscous flow*: The Bingham yield strength in the equation above, is made dependent on the normal stress:

$$\tau = \gamma\ H_i \left(\cos \alpha + \frac{a_c}{g} \right)(1 - r_u)\tan \phi$$

7. *Voellmy fluid*: The expression for T contains a Coulomb friction coefficient, μ, and a «turbulent friction» coefficient, ξ, as introduced by Voellmy (1955):

$$T = A_i \left[\gamma\ H_i \left(\cos \alpha + \frac{a_c}{g} \right)\tan \phi + \gamma\, \frac{v_i^2}{\xi} \right]$$

The rheological function and the material parameter values can vary along the slide path or within the slide mass for overriding of liquefiable soil or changes in pore pressure. The model allows for internal rigidity of relatively coherent slide debris moving on a thin liquefied basal layer.

To approximate a three-dimensional flow with an irregular cross-section, B_i can be taken as the top surface width and H_i is the hydraulic depth, defined as the ratio of the flow cross-sectional area divided by the top width. The surface width along the slide path is a prescribed input function. The flow resistance is assumed to act on the channel base only, while in reality it acts on the wetted perimeter of the channel. The value of the resulting error normally remains less than 10%. A second error results from the use of a constant width at any location, irrespective of the current flow depth. This error will affect the flow front and tail profile in cross-sections with sloping sides where the surface width should vary with depth. Given the moderate overall accuracy of run-out predictions, possible improvements are not considered productive. According to the author, the model represents a reasonable approximation to the three-dimensional confinement effects for all but very narrow channels. However, energy losses due to sudden constrictions or abrupt changes of cross-section or flow direction are not presently accounted for.

The importance of the lateral pressure coefficient, k, is clearly demonstrated by simulating a rock slide moving against a steep adverse slope. As observed by Hungr, «the model is shown to compare favourably with results of controlled laboratory experiments and other analytical tools (i.e. numerical models) for several different materials and problem configurations (including sudden breach of a tailings dam» (the comments within parentheses are those of the writer). Several examples, also including practical use, are presented. The

Computational models for dense snow avalanche motion

Report No: 581250-3
Date: 1996-04-30
Rev:
Rev. date:
Page: 22

model has been calibrated for flowslides from coal waste dumps by Kent and Hungr (1995).

10 THE BREITFUSS-SCHEIDEGGER DISPERSIVE PRESSURE MODEL

The model of Breitfuss and Scheidegger (1974) was originally developed for calculation of the shear velocity of debris flow motion. However, it is included in the present survey of avalanche models as it elucidates the distinction between the inertial and the macro-viscous regime, and because it is a particle model including «dispersive pressure». All these terms are also important to an understanding of avalanche motion (cf. the NIS and Kumar models below).

Breitfuss and Scheidegger (1974) state that the mechanism of debris flow is an intermediate process between bed load transport flow in rivers and suspension flow of, for example, powder snow avalanches. They state that the fluidization mechanism of debris flows is the one described by Bagnold (1954), where a «dispersive pressure» is present normal to the shearing direction because of particle interactions (inertial regime) or because of the influence of the grains on the flow patterns of the fluid around neighbouring grains (macro-viscous regime). It is the dispersive pressure that counteracts gravity and thus holds a mixture of water and debris in a fluidized state.

According to Bagnold (1954), one has a macro-viscous regime when

$$N = \frac{\lambda^{1/2} \sigma \, D^2 \, dU / dy}{\eta} < 40$$

and an inertial regime when $N > 450$, with a transition zone for $40 < N < 450$. $\lambda = \left((c_0 / c)^{1/3} - 1 \right)^{-1}$ is a measure of «packing», c is the actual and c_0 the maximum possible volume concentration of the grains (equals 0.74 for spheres), D and σ is the diameter and the density of the grains respectively and η is the kinematic viscosity of the continuous phase consisting of the water including the fine suspensions; dU / dy is the shear velocity.

Assumption of steady flow conditions for a balance between shear stresses due to the dispersive stresses parallel to the slope as expressed by Bagnold (1954) and shear stresses due to gravity, yields for the shear velocity at distance y above the bed in the inertial regime

$$\frac{dU}{dy} = \frac{1}{\lambda D} \left(\frac{\rho + (\sigma - \rho) c}{0.0128 \sigma} g(h - y) \sin \beta \right)^{1/2}$$

and in the macro-viscous regime

Computational models for dense snow avalanche motion

Report No: 581250-3
Date: 1996-04-30
Rev:
Rev. date:
Page: 23

$$\frac{dU}{dy} = \frac{[\rho + (\sigma - \rho)c]g(h-y)\sin\beta}{(1+\lambda)(1+\lambda/2)\eta}$$

where h is the flow height, g is the acceleration of gravity, β is the slope angle and ρ is the density of the continuous phase.

Examples for computation of dU/dy, and for the velocity U at the surface, are presented with actual choices of parameter values for the inertial regime. A check whether the regime is indeed the inertial one is also included.

11   THE YOSHIMATSU ENERGY DISSIPATION RESISTANCE MODEL

The Yoshimatsu (1991) model is originally a deformable body model for calculation of the vertical velocity profile of soil movement. However, it is included in the present survey of avalanche models because it is a particle model including the concept of «dynamic shear», which is also important in the understanding of avalanche motion (cf. the NIS and Kumar models below). The included shear stresses are caused by interparticle friction and inelastic collision of particles, i.e. dynamic shear. The former is proportional to the normal stresses (dry friction approach) while the latter is derived from a particle array model describing the energy dissipation by particle collision (Bagnold, 1954). Assumption of steady flow conditions by balance between shear forces and gravitational forces, yields for the velocity of dry sand in a distance y normal to the slope

$$u(y) = \frac{2}{3}\left(\frac{cg(\sin\theta - \mu\cos\theta)}{\frac{\pi\sigma}{12b}\sin^2\alpha\,(1-e^2)D^2}\right)^{1/2}\left(H^{\frac{3}{2}} - (H-y)^{\frac{3}{2}}\right)$$

whence the mean velocity is

$$\bar{u} = \frac{2}{5}\left(\frac{cg(\sin\theta - \mu\cos\theta)}{\frac{\pi\sigma}{12b}\sin^2\alpha\,(1-e^2)D^2}\right)^{1/2}H^{\frac{3}{2}}$$

where c is the volume concentration of the particles, g is acceleration of gravity, θ is the inclination of the slope, μ is the dynamic dry friction coefficient, H is the flow height, b is the average ratio of the distance between adjacent grains to the diameter D of the grains, α is some unknown angle determined by the collision conditions including grain rotation, σ is the density of the grains and e is coefficient of restitution for the particle collisions.

Computational models for dense snow avalanche motion

Report No: 581250-3
Date: 1996-04-30
Rev:
Rev. date:
Page: 24

NGI

Yoshimatsu (1991) also presents experimental methods to measure the static dry friction coefficient, and proposes that the ratio of the dynamic dry friction coefficient to the static dry friction coefficient is 0.8. He also discusses observed velocity and concentration distributions. The latter distributions are used to express the value of b in terms of c.

The numerical simulations presented for run-out distance and depositional shape are based on one-dimensional (depth-integrated) equations of continuity and momentum including erosion, where the shear stresses are implemented as described above. The equations are solved by finite differentiation.

Comparisons between experimental and calculated velocity profiles are presented, and according to the author «a satisfactory degree of coincidence was observed for the sedimentation process of dry sand through comparison with experimental results».

12 THE NIS VISCO-ELASTIC PLASTIC DEFORMABLE BODY MODEL

The NIS-model (Norem, Irgens and Schieldrop, 1987, 1989, Norem and Schieldrop, 1991) was originally developed for avalanches and has also been applied to submarine flowslides. Thus it is constructed to treat both kinds of energy dissipation regimes outlined in sections 1 and 10. The mathematical deformable body model describes a two-dimensional, non-steady shear flow of varying height with slip velocity conditions when erosion is omitted, or with no-slip velocity conditions when erosion is included. The shear flow moves along an arbitrary path originating centrifugal forces. The constitutive relations, which contain the visco-elasticity of a CEF-fluid (Criminale-Ericksen-Filbey, 1958) combined with plasticity for a cohesive material, yield (as depicted in Fig. 12.1) for the normal stresses σ_x and σ_y parallel and normal to the slope respectively, and for the shear stress τ_{xy}:

$$\sigma_x = p_e + p_u - \rho\,(\upsilon_1 - \upsilon_2)\left(\frac{dv_x(y)}{dy}\right)^r$$

$$\sigma_y = p_e + p_u + \rho\,\upsilon_2\left(\frac{dv_x(y)}{dy}\right)^r$$

$$\tau_{xy} = a + p_e \tan\varphi + \rho\,m\left(\frac{dv_x(y)}{dy}\right)^r$$

where p_e is the effective pressure (all normal compressive stresses have a positive sign according to soil mechanic practice), p_u is the pore pressure, ρ is the average density of the flowing material, υ_1 and υ_2 are the normal stress

Computational models for dense snow avalanche motion

Report No: 581250-3
Date: 1996-04-30
Rev:
Rev. date:
Page: 25

NGI

viscosities, $dv_x(y)\,/\,dy$ is the shear velocity parallel to the slope at a height y above the bed, a is the cohesion, φ is the internal friction angle, m is the shear stress viscosity and r is an exponent preliminary suggested equal to 2 for rock slides and avalanches (inertial regime) and 1 for debris flows of low concentration and submarine flowslides (macro-viscous regime).
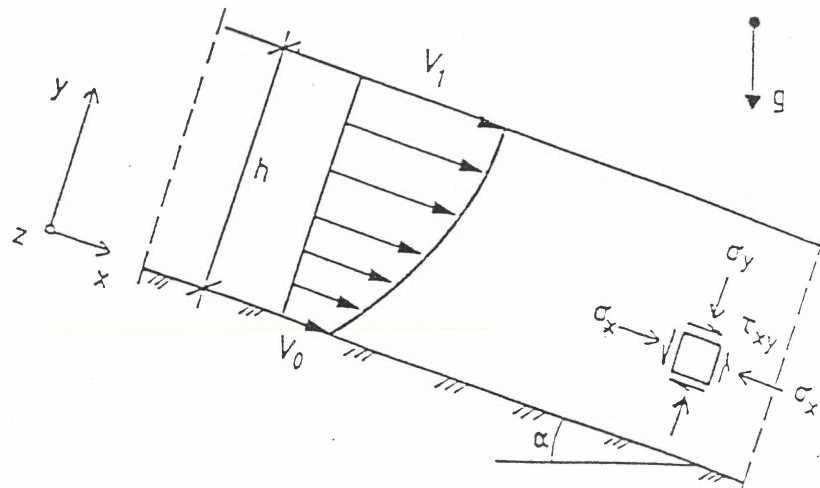

Fig. 12.1:   *Definition of steady flow geometry (after Norem, Locat and Schieldrop, 1989).*

As the viscometric functions are represented by power laws, they express flow induced dispersive pressure and dynamic shear, as described by Bagnold (1954). The model is quasi two-dimensional as the vertical velocity profile is assumed to be identical in form to the steady shear flow profile. Cohesion and/or upper surface shear stress induce a plug flow velocity profile, as opposed to the parabolic flow profile of a non-cohesive material with zero shear stress along the upper surface.

Cohesion, upper surface shear stress and erosion are omitted in the numerical model. The resulting partial differential equations are solved by a Eulerian finite-difference mid-point scheme in space and a fourth-order Runge-Kutta procedure in time.

The rear and frontal grid cells in the finite-difference representation of the avalanche are considered equal to the other cells in between. Each time the accumulated volume (i.e. volume flux integrated in time) passing through the contemporary avalanche front (i.e. the foremost «wall» of the frontal grid cell) matches the volume of the grid cell ahead of the avalanche (i.e. product of contemporary avalanche front height and grid distance), the avalanche is said to advance one grid distance. Similarly the rear grid cell is empty and neglected when the accumulated volume flowing out of the cell equals the volume

Computational models for dense snow avalanche motion

Report No:	581250-3
Date:	1996-04-30
Rev:	
Rev. date:	
Page:	26

NGI

contained in the cell when it was first defined to be the rear one, as the one behind was emptied.

To simplify comparison with other models, four program options are implemented:
- varying flow height and slip velocity conditions
- varying flow height and no-slip velocity conditions
- varying flow height and uniform profile
- constant flow height and velocity profile

The latter is approximately equal to the Voellmy or PCM models.

Several input parameters are needed: most important are the material friction coefficient (equals $\tan\varphi$) and the initial flow height h of the avalanche, cf. Table 19.1. For avalanches a default value, h_{crit}, is presented for the latter (Bakkehøi and Norem, 1994), based upon the fact that an unstable situation occurs when the actual shear stress, $\tau = \rho gh \sin\theta$ equals the yield strength, $\tau_y = a + \tan\varphi\rho gh\cos\theta$, of the snow:

$$h_{crit} = \frac{a}{\rho g(\sin\theta - \tan\varphi\cos\theta)}$$

where g is the acceleration of gravity and θ is the slope angle. The cohesion is eliminated by introducing a known reference height, $h_{40}=1.3$m, for a slope angle of 40°:

$$h_{crit} = h_{40}\frac{\sin 40 - \tan\varphi\cos 40}{(\sin\theta - \tan\varphi\cos\theta)}$$

A value of $\tan\varphi=0.3$ ($\varphi=17°$) is applied in the computations.

Bakkehøi and Norem (1994) also suggest that the length of the initial avalanche slab should equal one sixth of the total height difference of the slide path, with a maximum of 100 m.

The numerical results are verified by comparing with laboratory (Norem et al., 1992) and full-scale experimental data of avalanches (Norem, Irgens and Schieldrop 1989, Norem, 1992b), submarine slides (Norem, Locat and Schieldrop, 1989) and rock slides (Locat et al., 1992). For avalanches and submarine slides, the front velocity and the run-out distance are simulated well by the model. With varying flow height, the program is less sensitive to the shape of the path, and the computed deposits in the run-out zone also agree fairly well with experimental data.

Computational models for dense snow avalanche motion

Report No: 581250-3
Date: 1996-04-30
Rev:
Rev. date:
Page: 27

NGI

It is an admitted weakness by the authors that the model does not include effects of temperature and volume changes due to altering arrangements of the grains. Neither is the effect of active and passive earth pressure included. However, this effect is probably not significant as the internal friction is low due to the dispersive stress (Norem, pers. comm., 1995).

13 HYDRAULIC UNSTEADY FLOW MODELS

The quasi two-dimensional hydraulic flow (deformable body) models by Kulikovskii and Eglit (1973), Gregoryan and Ostroumov (1977) and Brugnot and Pochat (1981) (all discussed by Hopfinger, 1983) were originally used for dense-avalanche flow. Depth-averaged and one-dimensional equations similar to those used for calculating unsteady flood waves have been developed by utilising the analogy with open-channel hydraulics. The assumptions of hydrostatic pressure and a horizontal free surface in the cross-stream direction, yield the following one-dimensional continuity and momentum equations including the possible effects of channelling, slope changes and entrainment:

$$\frac{\partial P}{\partial t} + \frac{\partial Q}{\partial t} = 0$$

$$\frac{\partial Q}{\partial t} + \frac{\partial (Q^2/P)}{\partial x} + gP\frac{\partial h}{\partial x}\cos\theta = gP\left(\sin\theta - \mu\cos\theta - \frac{fQ^2}{P^2R}\right)$$

where $P = \rho A$ is the concentration (A is the cross-sectional area), $Q = PU$ is the flux at position x and time t, U is the depth-averaged velocity, h is the flow depth, g is the acceleration of gravity, μ is the dry friction coefficient and f is the dynamic drag coefficient.

The jump conditions at the front are described as an hydraulic jump. In a reference frame fixed in a front moving with velocity U_f, assuming that the shock thickness (in the moving direction) is small so that pressure forces dominate gravitational forces, continuity and momentum give

$$U_f(P - P_s) = Q$$

$$Q(U_f - U) = \frac{g\cos\theta}{n+1}(Ph - P_sh_s)$$

where θ is the slope inclination, n=1 for unconfined flow and n=2 for semicircular or triangular gullies. Subscript 's' refers to the incorporated snow cover ahead of the leading edge (Brugnot and Pochat, 1981).

Brugnot and Pochat (1981) test the following form of snow density variation:

Computational models for dense snow avalanche motion

Report No: 581250-3
Date: 1996-04-30
Rev:
Rev. date:
Page: 28

NGI

$$\rho = \frac{\rho_0}{1 + \alpha(U - U_0)}$$

where ρ_0 is the density at rest, U_0 is the threshold speed at which ρ varies and α is the coefficient of variation. Subsequently they include a sensitivity analysis of the model and conclude that the results vary extremely, depending on the selected friction value, while the sensitivity of density is less distinctive. Widening and narrowing of the gully do not effect the avalanche velocity much, and breaks in slope are much more efficient. Depth of entrainment largely determines the zone in which the avalanche stops. Comparisons with the Voellmy model and experimental *in situ* results reveal satisfactory results.

14 THE MURTY AND ESWARAN INTERNAL ENERGY HYDRAULIC MODEL

Murty and Eswaran (1994a) describe the avalanche as a quasi two-dimensional hydrostatic flow (deformable body) along a gully, the geometry of which is described by the cross-sections perpendicular to the line of greatest inclination. Resistance to the flow is assumed to include both dry, laminar and turbulent (dynamic drag) friction. With these assumptions they derive the following one-dimensional equations for conservation of mass, momentum and energy respectively (Murty and Eswaran, 1994b):

$$\frac{\partial S}{\partial t} + \frac{\partial P}{\partial x} = 0$$

$$\frac{\partial P}{\partial t} + \frac{\partial}{\partial x}\left(\frac{P^2}{S}\right) + gS\cos\psi\frac{\partial h}{\partial x} = gS\sin\psi - f_r$$

$$\frac{\partial}{\partial t}(Su) + \frac{\partial}{\partial x}(Pu) = Vf_r$$

where t and x refer to time and distance along the path of inclination ψ, g is the acceleration of gravity, h is the avalanche thickness, V is the snow speed, S is the cross-sectional area multiplied by density, P = SV is the mass-flow rate and u is the specific internal energy of the snow. All the dependent variables, h, V, S, P and u, are functions of x and t. The frictional term f_r is

$$f_r = f_d gS\cos\psi + f_l g\frac{P}{R^2} + f_t g\frac{P^2}{SR}$$

where f_d, f_l and f_t are the coefficients of dry, laminar and turbulent friction respectively, and R is the hydraulic radius (equal to cross-sectional flow area divided by wetted perimeter).

Computational models for dense snow avalanche motion

Report No: 581250-3
Date: 1996-04-30
Rev:
Rev. date:
Page: 29

NGI

In general the geometrical relationship between cross-sectional flow area and h, the equation of state between u and temperature, and an equation that models the density as an empirical function of other flow variables such as velocity, temperature, etc. have to be added to the equations above. However, so far the authors assume that the density does not vary. Furthermore, in the presented example, $f_l=0.0$ (while $f_d=0.2$ and $f_t=0.02$).

The equations are solved numerically by the MacCormack method which is an explicit, second order and two level predictor corrector scheme capable of capturing shocks without isolating them. A no-flux boundary condition is imposed on the upstream end of the avalanche path, and a continuity boundary condition is applied at the downstream end.

15   THE KUMAR INTERNAL ENERGY HYDRAULIC MODEL

Kumar (1994) presents an extension of the Murty and Eswaran-model, incorporating the aspects of dispersive pressure and dynamic shear as in the NIS-model. The velocity at a distance y above the bed is given by

$$V(y) = V_1 - (V_1 - V_0)(1 - \frac{y}{h})^{1.5}$$

where V_1 is the velocity at the surface of the avalanche flow, V_0 is the slip velocity along the bed and h is the avalanche thickness. The effect of compressibility might be considered by describing the density in the equations in accordance with Brugnot and Pochat (1981), cf. sec. 13.

Hence the equations of balance of mass, linear momentum and energy expressed in terms of maximum velocity V_1 are:

$$\frac{\partial(\rho A)}{\partial t} + \frac{\partial(\rho A V_1 \alpha_1)}{\partial x} = 0$$

$$\frac{\partial(\rho A V_1 \alpha_1)}{\partial t} + \frac{\partial(\rho A V_1^2 \alpha_2)}{\partial x} + \rho A \left[g \cos\theta - \frac{9\upsilon_1}{4R_h^3} V_1^2 (1 - R_v)^2 \right] \frac{\partial h}{\partial x}$$

$$= \rho g A \sin\theta - b\rho g A \cos\theta - \frac{9\rho A}{4R_h^3}(m - b\upsilon_2)V_1^2(1 - R_v)^2$$

$$\frac{\partial(\rho A u)}{\partial t} + \frac{\partial(\rho A V_1 u \alpha_1)}{\partial x} = V_1 \alpha_1 (b\rho g A \cos\theta + \frac{9\rho A}{4R_h^3}(m - b\upsilon_2)V_1^2(1 - R_v)^2$$

Computational models for dense snow avalanche motion

Report No: 581250-3
Date: 1996-04-30
Rev:
Rev. date:
Page: 30

NGI

where A is the cross-sectional area of the path, u is the specific internal energy and ρ is the snow density at time t and position x along the path of inclination θ, while g is the acceleration of gravity, m is the shear viscosity, υ_1 and υ_2 are the normal stress viscosities, b is the Coulomb friction coefficient, R_h is the hydraulic mean radius and $R_v = V_0 / V_1$. According to the author introduction of the correction factors $\alpha_1 = (\int_A V(y)dA) / V_1 A$ and $\alpha_2 = (\int_A V^2(y)dA) / V_1^2 A$ for mass flow rate and momentum respectively, gives more realistic values for these variables.

The third term on the left-hand side of the momentum equation represents the normal force over the cross-section due to effective and dispersive pressure, while the two latter terms on the right hand side represent shear force due to Coulomb friction and dynamic shear.

The equations are solved numerically in the same way as in the preceding Murty and Eswaran-model.

16 THE HUTTER, SAVAGE, NOHGUCHI AND KOCH GRANULAR DEFORMABLE BODY MODEL

Hutter and Koch (1991) describe a model to predict the flow of an initially stationary mass of cohesionless granular material (rock, ice and dense flow avalanches) obeying a Coulomb-type internal friction down a rough curved bed. They apply the depth-averaged non-linear one-dimensional equations of balance of mass and linear momentum (Savage and Hutter, 1990), which in dimensionless forms are written

$$\frac{\partial h}{\partial t} + \frac{\partial (hu)}{\partial x} = 0,$$

$$\frac{\partial u}{\partial t} + u \frac{\partial u}{\partial x} = \sin \zeta - \tan \delta \, sgn(u)(\cos \zeta + \lambda \kappa \, u^2) - \varepsilon \, K_{ap} \cos \zeta \frac{\partial h}{\partial x}$$

The first equation is exact, while the latter one introduces relative errors of order ε^2=(depth scale/longitudinal length scale)^2; u is the depth-averaged velocity at position x and time t, h is the flow height, ζ is the slope angle, δ is the (non-constant) bed friction angle, λ= (longitudinal length scale/scale for the radius of curvature of the bed profile), κ is the curvature and K_{ap} is the earth pressure coefficient that can take active or passive values according to whether $\partial u / \partial x$ is positive or negative. When $\tan\delta$ and/or λ are smaller than order $\varepsilon^{1/2}$, and u does not become too large (upper limit not specified), then the term in the momentum equation due to centrifugal effects may be dropped. Since ζ may

Computational models for dense snow avalanche motion

Report No: 581250-3
Date: 1996-04-30
Rev:
Rev. date:
Page: 31

still vary with position, some weak curvature effects are still implicitly incorporated. The equations are solved numerically by a Lagrangian finite difference scheme that incorporates numerical diffusion (Savage and Hutter, 1989). Hutter and Koch (1991) analyse the reliability of this scheme when the numerical diffusion is varied (a conventional Eulerian finite difference scheme was first unsuccessfully attempted).

For granular flows which start as parabolic piles, the governing equations (incorporating weak curvature effects) permit similarity solutions (Savage and Hutter, 1989, Savage and Nohguchi, 1988, Nohguchi et al., 1989 and Hutter and Nohguchi, 1990). These are approximate solutions of the equations above because the centrifugal force term is ignored and the variation of the slope angle ζ within the moving pile is replaced by a first-order Taylor series expansion about the centre of gravity. Savage and Nohguchi (1988) show that the motion of the centre of mass of the parabolic pile and its spread can be derived from a set of ordinary differential equations that must be solved numerically. The parabolic shape is preserved and the velocity distributions are simple.

Savage and Hutter (1989) found previously similarity solutions for granular flow down an inclined flat bed. They showed that the parabolic pile spreads linearly in time and its height decreases as t^{-1} when $t \rightarrow \infty$. They also found the solution for an M-wave, i.e. a pile with cliff-like edges and smaller depths towards the middle of the moving mass. Its spread grows as $t^{2/3}$ and its height decreases as $t^{-2/3}$ when $t \rightarrow \infty$. Stability analysis shows rigorously that both solutions are stable against small perturbations. A Eulerian scheme is able to reproduce the M-wave similarity solution quite well, while a Lagrangian scheme must be introduced for the parabolic pile shape.

Hutter and Koch (1991) further present laboratory experiments with various materials and bed linings. Angle of repose and bed friction angle are determined. The effect of chute walls is incorporated in an effective bed friction angle that showed a linear dependence on the pile depth. Both the general equation model and the similarity model are compared with the experimental results. Satisfactory agreement between the general equation model and the laboratory experiments is obtained if the internal angle of friction, ϕ, exceeds the total bed friction angle, δ (otherwise erosion might occur and a depth-averaged model is not appropriate), or is not close to it. Limited variations of δ along the bed do not seem to have significant effect on the computational results. It is important to use dynamic values for ϕ and δ. For the similarity solution model no initial condition can be found that yield computational results for the position of the leading and trailing edges of the granular flow in sufficient agreement with the observations. However, when depth-to-length ratio of the initial pile geometry and the curvature of the bed are sufficiently small, this model may be used for diagnostic purposes.

Computational models for dense snow avalanche motion

Report No: 581250-3
Date: 1996-04-30
Rev:
Rev. date:
Page: 32

NGI

17 THE LANG AND LEO THREE-DIMENSIONAL GRANULAR DEFORMABLE BODY MODEL

Lang and Leo (1994) have developed a quasi three-dimensional deformable body model to describe the motion of dense avalanches, ice and rock slides. The slide masses are described as an incompressible cohesionless granular media obeying a Coulomb-type yield criterion moving down an open terrain of variable curvature in the longitudinal direction. The basal bed friction is described similarly by a Coulomb friction. An «earth pressure coefficient» is included. Lateral variations in topography and changes in volume fraction of granulate are neglected. The mass is assumed to retain a lateral parabolic shape. This assumption is supported by experimental results reported by Lang et al. (1989). The model is an extension into three spatial dimensions of that by Hutter et al. described above. In addition a boundary drag term proportional to the velocity squared is included, as the analytical results indicate the existence of a flow transition regime analogous to a laminar to turbulent transition in a fluid.

A non-dimensional scheme is employed, choosing three characteristic length scales. The depth- and width-averaged three-dimensional balance equations including sidewise spreading of the mass are solved by a Lagrangian finite difference scheme (Savage and Hutter 1989). With this method, the boundaries of the computational grid is convected with the depth- and width-averaged velocities. An artificial viscosity term $\mu \dfrac{\partial^2 u}{\partial x^2}$ is added to the equation of motion in order to smooth the solution.

According to the authors, kinematic theories predict quadratic dependence of stress on shear-rate, for rapidly shearing highly dispersed material, in good agreement with available laboratory data. The authors further state that this extreme case may be used to describe the behaviour of the dust cloud, which does not represent any type of snow avalanche activity that could be construed as destructive, and need not be considered.

This does not agree with the theory of Bagnold (1954), in which there is a linear dependence of stress on shear-rate at low solid concentrations (e.g. snow dust cloud) when energy dissipation is caused mainly by viscosity in the interstitial fluid (macro-viscous regime), while there is a quadratic dependence at high solid concentrations (e.g. dense snow avalanches) when energy dissipation is caused by particle interactions. The latter connection has proved to be important for the NIS-model described above. Besides dust clouds, or rather powder avalanches, might be severely destructive.

The numerical simulations are compared to experimental results by Lang et al. (1989), in plots of position and velocity versus time as well as width and height versus length. Contour or three-dimensional perspective plots are missing. The

Computational models for dense snow avalanche motion

Report No: 581250-3
Date: 1996-04-30
Rev:
Rev. date:
Page: 33

NGI

constant bed friction angle model is good for experiments with a starting zone angle of 35°. For greater starting zone angles, the model greatly overestimates the run-out distance, probably because a transition in flow regime occurs in the boundary layer where the boundary drag becomes non-negligible. When a linear combination of a constant bed friction and a boundary drag is applied, the model reflects well the general motion of the mass, and the authors state that the results justify the characterisation of the flow, and pursuance of averaged quantities. However, the maximum leading edge velocity is not attained by the model. Ideally, the boundary drag term should perhaps be included only when a critical velocity is attained.

The authors admit that some subjectivity is still required to determine constitutive parameters, and it is unknown if the models can represent naturally occurring events. Future work should include testing against natural events, determining the importance of topographical variations in the lateral direction, cohesion and particle size distribution.

18 THE TAKAHASHI AND YOSHIDA/HUNGR AND MCCLUNG LEADING-FRONT RUN-UP MODEL

The traditional method of calculating avalanche run-up heights pioneered by Voellmy (1955) is based on the law of conservation of energy, including frictional energy losses, when modelling the flow as a point mass. According to McClung (1990), turbulent friction is not significant in most problems of interest with respect to run-up. Hence, including only a Coulomb-type basal resistance, the solution for the run-up height is

$$H_v = \frac{U_0^2 \sin \theta}{2g(\mu \cos \theta - \sin \theta)}$$

where U_0 is speed entering the run-up segment, θ is the inclination of the run-up barrier, g is the acceleration of gravity and μ is the dynamic Coulomb friction coefficient.

Perla et al. (1980) replaced U_0 by $U_0 \cos(\theta_0 - \theta)$ for conservation of linear momentum at the slope transition upstream of the run-up barrier, giving the corrected run-up height estimate

$$H_{vc} = \frac{U_0^2 \cos^2(\theta_0 - \theta) \sin \theta}{2g(\mu \cos \theta - \sin \theta)}$$

where θ_0 is the inclination above the slope transition.

Computational models for dense snow avalanche motion

Report No: 581250-3
Date: 1996-04-30
Rev:
Rev. date:
Page: 34

Hungr and McClung's (1987) reformulation of the run-up equation by Takahashi and Yoshida (1979, see Takahashi, 1991, for English version), allowed a calculation of the run-up of dry avalanches by considering the forces responsible for driving the front of the avalanche up the barrier with most of the mass remaining behind. Their one-dimensional expression for the time rate of change of the leading front momentum is given by

$$\frac{d(h\rho\, Ux)}{dt} = T_1 + T_2 + T_3 + T_4$$

where h is the flow height of the front, x is the avalanche length along the barrier at time t, U is the depth averaged speed of the avalanche front and ρ is the depth averaged avalanche density (assumed constant); $T_1 = \rho\, ghx \sin\theta$ is the gravity driving force, $T_2 = \rho\, h_0 U_0^2 \cos(\theta_0 - \theta)$ is the momentum flux between the body of the avalanche with height h_0 and its front, assuming both steady momentum supply at the toe of the barrier and supercritical flow so that the barrier does not influence the conditions upstream, $T_3 = \frac{1}{2}\rho\, gh_0^2 \cos\theta_0 \cos(\theta_0 - \theta)$ is the granular flow thrust force between the avalanche body and the front, analogous to depth averaged hydrostatic pressure, and $T_4 = \mu\rho\, ghx \cos\theta$ is the basal Coulomb friction force.

By also invoking the continuity equation

$$hx = h_0 U_0 t,$$

Takahashi (1991) and Hungr and McClung (1987) provide the following solution for the run-up height:

$$H = \frac{U^{*2} \cos^2(\theta_0 - \theta)\sin\theta}{g(\mu\cos\theta - \sin\theta)}$$

where

$$U^* = U_0\left(1 + \frac{gh_0 \cos\theta_0}{2U_0^2}\right)$$

Note that the solution depends only on the incoming flow depth h_0, and not on the frontal depth h. If the fluid thrust force T_3 is neglected, then $U^* = U_0$ and the latter expression for H gives exactly twice the run-up height H_{vc} predicted by Perla et al. (1980) above. This is because the point mass model considers the entire mass to be lifted to height H_{vc}, and hence underestimates the run-up height compared to the leading front model, which requires only the front to be

Computational models for dense snow avalanche motion

Report No: 581250-3
Date: 1996-04-30
Rev:
Rev. date:
Page: 35

lifted to height H. Hungr and McClung (1987) showed that the comparison changes very little if turbulent drag proportional to U^2 is considered.

Experimental results by Chu et al. (1994) reveal that the fluid thrust force T_3 is negligible, and that the run-up height H_v based on Voellmy's (1955) approach without momentum loss at the slope transition is significantly overestimated (the opposite effect occurs if the approach angle θ_0 is close to zero). The Hungr-McClung theory (1987) provides excellent results in the intermediate range ($\theta=30°$) relevant for avalanche barriers constructed of earth materials.

When the slope transition approaches $90°$, the maximum run-up height is determined by material that overrides that deposited previously at the bend. Neither model contains this «self-ramping» effect.

19 EXAMPLES OF RUN-OUT DISTANCE CALCULATIONS

Four Norwegian avalanche events have been back-calculated by the statistical two-parameter α/β-model, the comparative model and by the three numerical dynamic models available to the author: PCM, NIS and VSG, see Table 19.1.

As stated above, the results of the dynamic models can be tuned by the choices of input parameter values to obtain agreement between observed and calculated run-out distances. Thus the intention here is not to evaluate or range the dynamic models, which is not possible from observations of run-out distance only, but rather to illustrate what input parameter values must be selected to obtain the desired run-out distances of the avalanches.

All of the four back-calculated events are located in the Northwest part of Southern Norway, as most events in the avalanche database of NGI. Starting point elevation varies from 960m to 1400m a.s.l., while stopping point elevation varies from 5m to 45m a.s.l. The first three events in Table 19.1 have unconfined track zones, while the track zone of the fourth event is a V-shaped gully.

The results of the statistical two-parameter α/β-model deviate by $-1.0°$ to $+3.0°$ from the observed run-out angle, i.e. -0.4 to +1.3 standard deviations. The results of the comparative model are slightly worse, deviating by $-1.1°$ to $+4.4°$ from the observed run-out angle.

For the three dynamic models, combinations of parameter values are selected based on previous experience with the models to obtain less than 20m difference between observed and calculated values. Table 19.1 reveals that the selected combinations of parameter values for the dynamic models agree surprisingly well between the last three events, while friction coefficients and viscosities have to be significantly greater, and initial flow height has to be smaller, for the first event.

Computational models for dense snow avalanche motion

Report No: 581250-3
Date: 1996-04-30
Rev:
Rev. date:
Page: 36

For the PCM-model the dry friction coefficient, μ, is varied under the restriction that the mass-to-drag ratio, M/D, should vary between 400m^{-1} and 1200m^{-1}. Each enhancement of $200\ \text{m}^{-1}$ in the mass-to-drag ratio, requires a corresponding increase in the dry friction coefficient of 0.02-0.03 to obtain a similar run-out distance. If not only the run-out distance of each event is considered, but also the maximum avalanche velocity, it is possible to some extent to restrict the range of parameter values. Velocity measurements from the full-scale avalanche experimental site Ryggfonn in Southern Norway (Norem, 1995b), indicate that even large avalanches of more than 100.000m^{3}, do not reach higher velocities than about 60m/s. Thus a mass-to-drag ratio of 1200m^{-1} seems to be too high for the PCM-model. Correspondingly a ratio of 400m^{-1} for the first event reveals a too small velocity. Hence $0.05 \leq \mu \leq 0.35$ ($0.05 \leq \mu \leq 0.15$ for the last three events), and $600\,\text{m}^{-1} \leq M/D \leq 1000\,\text{m}^{-1}$ should be convenient parameter values for the PCM-model.

For the NIS-model the first combination of parameter values for each event includes the default value of the initial flow height. Thereafter the initial flow height is increased 0.5m at a time, while either the material friction coefficient or the shear stress viscosity (or both to avoid too great changes in each individual one) is altered correspondingly. Within the selected range of initial flow heights, adding 0.5m corresponds to an increment of 25-38% between those pairs of cases where only one other parameter value is altered. To sustain agreement between observed and calculated run-out distance, the increase in flow height, h, implies an addition to the material friction coefficient, $\tan\varphi$, of 10-40% or an addition to shear stress viscosity, m, of 27-120%. Hence the model is more sensitive to the values of h and $\tan\varphi$ than to the values of m. The maximum avalanche velocities indicate that $0.14 \leq \tan\varphi \leq 0.35$ ($0.14 \leq \tan\varphi \leq 0.25$ for the last three events) and $0.0005 \leq m \leq 0.0016$ are convenient parameter values for the NIS-model.

For the VSG-model, the dry friction coefficient is selected in agreement with that of the PCM-model in the first event. Also here the initial flow height is increased 0.5m at a time. The combinations of parameter values for the last three events are restricted by the fact that the program does not accept a dry friction coefficient, μ, less than 0.15 or a turbulent friction coefficient, ξ, greater than 1500m/s^{2}. Adding 0.5m to the initial flow height, d_0, here corresponds to an increment of 16.7-33.3%, and implies a reduction in ξ of 10-23%. It is difficult to utilise avalanche velocities to restrict the range of parameter values for the VSG-model, since the program returns only the terminal velocity at the bottom of the track, and not the maximum velocity.

A more thorough analysis of parameter values and accuracy of the five models mentioned above can be found in Bakkehøi et al. (1983) and Lied et al. (1995).

Table 19.1 Observed and calculated run-out distances with examples of parameter value combinations for four Norwegian avalanches. R_{obs} and R_{calc} is observed and calculated run-out distance respectively, α_{obs} and α_{calc} is observed and calculated run-out angle respectively, v_{max} is maximum velocity, v_{term} is terminal velocity at the bottom of the track, other symbols explained in the text for each model.

	α/β		Comparative	PCM				NIS						VSG				
	β (deg.)	α_{calc} (deg.)	α_{calc} (deg.)	μ	M/D (m⁻¹)	v_{max} (m/s)	R_{calc} (m)	$\tan\varphi$	m (m²)	h (m)	α_{calc} (deg.)	v_{max} (m/s)	R_{calc} (m)	μ	ξ (m/s²)	d_0 (m)	v_{term} (m/s)	R_{calc} (m)
SKAFONNA, NORDDAL 1922 α_{obs}=28° R_{obs}=2545m	29.6	27.0	26.9	0.25	400	38.1	2530	0.30	0.0011	1.30	27.9	39.2	2545	0.25	650	1.50	26.7	2555
				0.28	600	43.4	2550	0.25	0.0015	1.30	27.9	37.2	2535	0.25	500	2.00	27.0	2550
				0.30	800	47.0	2565	0.35	0.0015	1.80	27.6	45.8	2575	0.30	1000	1.50	30.4	2560
				0.35	1000	47.4	2525	0.35	0.0019	1.80	28.0	42.4	2530	0.30	800	2.00	31.4	2570
KORSBREKK-FONNA, STRANDA 1942 α_{obs}=32° R_{obs}=1520m	37.9	35.0	36.4	0.05	600	60.0	1540	0.20	0.0005	1.52	32.0	63.0	1520					
				0.08	800	65.2	1525	0.20	0.0011	2.00	32.0	62.3	1520	0.15	1500	1.50	33.2	1540
				0.10	1000	69.9	1535	0.22	0.0011	2.50	32.2	65.1	1515	0.15	1200	2.00	34.3	1550
				0.12	1200	73.3	1535											
KORSAFONNA, ØRSTA 1968 α_{obs}=24.5° R_{obs}=2612m	28.2	25.7	26.3	0.07	600	52.9	2625	0.14	0.0005	1.08	24.5	47.7	2610					
				0.11	800	58.0	2615	0.20	0.0009	1.50	24.5	56.1	2615	0.15	1500	1.75	37.0	2615
				0.15	1000	61.2	2600	0.30	0.0011	2.00	24.5	66.4	2615	0.15	1200	2.25	37.5	2610
				0.18	1200	63.7	2600	0.25	0.0016	2.00	24.5	61.2	2610					
SKONDALS-FONNA, ØRSTA 1882 α_{obs}=19.8° R_{obs}=3445m	23.7	21.4	22.5	0.04	600	49.8	3460	0.23	0.0005	1.30	19.8	68.3	3445					
				0.07	800	55.1	3440	0.26	0.0011	1.80	19.9	69.4	3430	0.15	1500	2.50	43.7	3460
				0.10	1000	58.6	3420	0.31	0.0011	2.30	19.9	71.3	3430	0.15	1350	3.00	43.8	3455
				0.12	1200	61.6	3440	0.28	0.0019	2.30	19.9	70.5	3430					

Computational models for dense snow avalanche motion

Report No: 581250-3
Date: 1996-04-30
Rev:
Rev. date:
Page: 38

NGI

20   CONCLUDING REMARKS

Seventeen various models for the computation of avalanche motion have been discussed. The models include statistical, comparative and energy considering methods for run-out distance computations, in addition to different approaches for describing the dynamic behaviour of the moving masses.

The dynamics of avalanches are complex, involving both fluid, particle and soil mechanics. A favourable and universal model does not exist. In particular, there is scope to further develop the dynamic models.

Field observations of avalanches are difficult to make and yield only limited information. Nevertheless measurements of flow height, density and vertical velocity gradients, front velocity, etc. along the slide path would increase the understanding of the mechanisms involved and would be helpful in evaluating the dynamic models. At present, several models with different descriptions of the dynamics and the material properties can all provide the deficient recorded observations from one certain event by tuning of parameter values. Thus, all predictions of run-out distance, impact pressure, etc. for a possible event are based on a high degree of subjective judgement and experience, and hence are encumbered with uncertainty.

Density variations are simply represented in only a very few models, while the resultant effects on other physical parameter values such as viscosity, are not represented in any of the dynamic models. Other aspects of the moving media, such as nonhomogeneous concentration, particle size distribution, cohesion, particle rotation as well as temperature changes and energy dissipation are not adequately described in any of the dynamic models. Furthermore there is a conspicuous lack of any description of stability and accuracy of the applied numerical methods.

A few (quasi) three-dimensional models already exist, and effort is now being made to expand more of the one- and two-dimensional models into three dimensions. However, it is the impression of the author that it is at least of equal importance to improve the two-dimensional models further, preferably by combining models based on Bagnold's (1954) concept of dispersive pressure and dynamic shear with granular flow models involving aspects of soil mechanics.

A closer collaboration between the scientific disciplines of avalanches, submarine slides, inclined gravity currents, granular flows, soil mechanics, landslides, and numerical analysis would be fruitful.

Computational models for dense snow avalanche motion

Report No: 581250-3
Date: 1996-04-30
Rev:
Rev. date:
Page: 39

NGI

ACKNOWLEDGEMENTS

21   REFERENCES

Alean, J. 1984
Untersuchungen über Entstehungsbedingungen und Reichweiten von Eislawinen. Mitteilung No. **74** der *Versuchsanstalt für Wasserbau, Hydrologie und Glaziologie an der Eidgenößischen Technischen Hochschule (Zürich).*

Alean, J. 1985
Ice avalanches: Some empirical information about their formation and reach. *Journal of Glaciology* Vol. **31**, No. **109**.

Bagnold, R.A. 1954
Experiments on a gravity free dispersion of large solid spheres in a Newtonian fluid under shear. *Proceedings of the Royal Society of London*, Ser. A**225**, 49-63.

Bagnold, R.A. 1956
The flow of cohesionless grains in fluids. *Phil. Transaction of the Royal Society of London*, **249**, 235-297.

Bakkehøi, S., Cheng, T., Domaas, U., Lied, K., Perla, R.I. and Schieldrop, B. 1981
On the computation of parameters that model snow avalanche motion. *Canadian Geotechnical Journal* **18**(**1**), 121-130.

Bakkehøi, S., Domaas, U. and Lied, K. 1983
Calculation of Snow Avalanche Run-out Distance. Annals of Glaciology, Vol. 4, 24-29. Also in: *Norwegian Geotechnical Institute*, publication no. **151**, 1984.

Bakkehøi, S. and Norem, H. 1993
Comparing topographical and dynamical run-out models by ideas of «Nearest Neighbour Method». *2nd Avalanche-Dynamics-Workshop in Innsbruck.* Preliminary.

Bakkehøi, S. and Norem, H. 1994
Sammenlikning av metoder for beregning av maksimal utløpsdistanse for snøskred (Comparing methods for calculation of maximum avalanche runout distance). *Norwegian Geotechnical Institute*, report **581200-30** (in Norwegian).

048. Bra-Trykk AS

Computational models for dense snow avalanche motion

Report No: 581250-3
Date: 1996-04-30
Rev:
Rev. date:
Page: 40

NGI

Breitfuss, G. and Scheidegger, A.E. 1974
On a possible mechanism of Alpine debris flows. *Annali di Geofisica*, **XXVII**, Nr. **1-2**, 47-57.

Brugnot, G. and Pochat, R. 1981
Numerical simulation study of avalanches. *Journal of Glaciology* Vol. **27**, No. **95**, 77-88.

Brørs, B. 1991
Turbidity current modelling. *Division of Structural Engineering, Norwegian University of Science and Technology,* Dr.Ing.-thesis 1991:**38**.

Buser, O. 1983
Avalanche Forecast with the Method of Nearest Neighbours. An Interactive Approach. *Cold Regions Science and Technology,* Vol. **8**, No. **2**, 155-163.

Buser, O., Bütter, M. and Good, W. 1987
Avalanche forecast by the nearest neighbour method. *IAHS*, publ. no. **162**.

Buser, O. and Frutiger, H. 1980
Observed maximum run-out distance of snow avalanches and the determination of the friction coefficients μ and ξ. *Journal of Glaciology* Vol. **26**, No. **94**, 121-130.

Chu, T., Hill, G., McClung, D.M., Ngun, R. and Sherkat, R. 1994
Experiments on granular flows to predict avalanche runup. *Canadian Geotechnical Journal* **32**, 285-295 (1995).

Criminale, W.O.Jr., Ericksen and Filbey,G.L. 1958
Steady Shear Flow of Non-Newtonian Fluids. *Archive Rat. Mech. Anal* **1**, 410-417.

Föhn, P. and Meister, R. 1982
Determination of avalanche magnitude and frequency by direct observations and/or with the aid of indirect snowcover data. *IUFRO/FAO collegium on research on small torrential watersheds (inc. avalanches),* June 1981, Grenoble, France.

Goldstein, H. 1980
Classical mechanics. Second edition. *Massachusetts, Addison-Wesley Publishing Company.*

Gregoryan, S.S. and Ostroumov, A.V. 1977
Mathematical simulation of the process of motion of a snow avalanche (summary only). *Journal of Glaciology* Vol. **19**, 664-665.

Computational models for dense snow avalanche motion

Report No: 581250-3
Date: 1996-04-30
Rev:
Rev. date:
Page: 41

Gubler, H.U. 1987
Measurements and modelling of snow avalanche speeds. *International Association of Hydrological Sciences Publication* **162** (Symposium at Davos 1986 - *Avalanche Formation, Movement and Effects)*, 405-420.

Gubler, H.U. 1993
Swiss Avalanche-Dynamics Procedures for Dense Flow Avalanches. *AlpuG, Dr. H. Gubler, Richtstattweg 2, CH-7270 Davos Platz.*

Harbitz, C. 1995
Flateyri, Island; Etterberegning av skredet 26 oktober 1995 (Back-calculation of the Oct. 26 1995 avalanche). *Norwegian Geotechnical Institute*, report **581250-1** (in Norwegian).

Harbitz, C. 1996
Computational models for rock slide and debris flow motion. *Norwegian Geotechnical Institute*, report **585910-6**.

Hermann, F. and Hutter, K. 1991
Laboratory experiments on the dynamics of powder-snow avalanches in the run-out zone. *Journal of Glaciology* Vol. **37**, No. **126**.

Hopfinger, E.J. 1983
Snow avalanche motion and related phenomena.
Ann. rev. Fluid Mech. 1983, **15**, 47-76.

Hungr, O. 1995
A model for the runout analysis of rapid flow slides, debris flows, and avalanches. *Canadian Geotechnical Journal* **32**, 610-623.

Hungr, O. and McClung, D.M. 1987
An equation for calculating snow avalanche run-up against barriers in avalanche formation, movement and effects. *Proceedings, Davos Symposium, 1986. International Association of Hydrological Sciences,* Publication **162,** 605-612.

Hutter, K. 1991
On flow of granular materials. *Lecture notes. Techn. Hochschule Darmstadt.*

Hutter, K. and Koch, T. 1991
Motion of a granular avalanche in an exponentially curved chute: experiments and theoretical predictions. *Phil. Trans. R. Soc. Lond. A* (1991) **334**, 93-138.

Hutter, K. and Nohguchi, Y. 1990
Similarity solutions for a Voellmy model of snow avalanches with finite mass.
Acta Mechanica **82**, 99-127.

Computational models for dense snow avalanche motion

Report No: 581250-3
Date: 1996-04-30
Rev:
Rev. date:
Page: 42

NGI

Kent, A. and Hungr, O. 1995
Runout characteristics of debris from mine waste dump failures in mountainous terrain. *Canada center for Mineral and Energy Technology, Edmonton, Coal Research Laboratories.*

Kulikovskii, A.G. and Eglit, M.E. 1973
Two-dimensional problem of the motion along a slope with smoothly changing properties. *PMM J. Appl. Math. Moch.* **37**, 792-803. Transl. from *Prikl. mat. Mekh.* **37**, 837-848.

Kumar, A. 1994
Continuum approach to avalanche dynamics. *Extended abstracts, Int. symp. on snow and related manifestations, Snow & Avalanche Study Establishment, Manali (HP), India,* Sep. 1994.

Körner, H.J. 1976
Reichweite und Gescwindigkeit von Bergsturzen und Fließschneelawinen. *Rock Mechanics* Vol. **8**, No. **4**, 225-256.

Körner, H.J. 1980
The energy line method in the mechanics of avalanches. *Journal of Glaciology* Vol. **26**, No. **94**, 501-505.

Lang, R.M. and Leo, R. 1994
Model for avalanches in three spatial dimensions - Comparison of theory to experiments. *Cold regions research and engineering laboratory* report **94-5**.

Lang, R.M., Leo, R. and Hutter, K. 1989
Flow characteristics of an unconstrained non-cohesive granular medium down an inclined, curved surface: Preliminary experimental results. *Annals of Glaciology* Vol. **13**, 146-153.

Lied, K. and Bakkehøi, S. 1980
Empirical Calculations of Snow-Avalanche Run-Out Distance Based on Topographic Parametres. Journal of Glaciology, Vol. 26, No. 94, 165-177. Also in: *Norwegian Geotechnical Institute*, publication no. **133**, 1981.

Lied, K. and Toppe, R. 1988
Calculation of maximum snow-avalanche run-out distance by use of digital terrain models. Annals of Glaciology, Vol. **13**, 1989, 164-169. Also in: *Norwegian Geotechnical Institute*, publication no. **183**, 1992.

Lied, K., Weiler, C., Bakkehøi, S. and Hopf, J. 1995
Calculation methods for avalanche run-out distance for the Austrian Alps. *Norwegian Geotechnical Institute*, report **581210-1**.

Computational models for dense snow avalanche motion

Report No: 581250-3
Date: 1996-04-30
Rev:
Rev. date:
Page: 43

NGI

Locat, J., Norem, H. and Therrien, P. 1992
An approach to rock avalanche dynamics. *Norwegian Geotechnical Institute*, report **585000-10**.

Martinelli, M. jr. 1986
A test of the avalanche runout equations developed by the Norwegian Geotechnical Institute. *Cold Reg. Sci. Technol.* **13** (**1**), 19-33.

Martinelli, M.Jr., Lang, T.E. and Mears, A.I. 1980
Calculations of avalanche friction coefficients from field data. *Journal of Glaciology* Vol. **26**, No. **94**, 109-119.

McClung, D.M. 1990
A model for scaling avalanche speeds, *Journal of Glaciology* Vol. **36**, No. **123**, 188-198.

McClung, D.M. and Lied, K. 1987
Statistical and geometrical definition of snow avalanche runout. *Cold Reg. Sci. Technol.,* **13** (**2**), 107-119.

McClung, D.M., Mears, A.I. and Schaerer, P. 1989
Extreme avalanche run-out: Data from four mountain ranges. *Annals of Glaciology* Vol. **13**, 180-184.

Mellor, M. 1978
Dynamics of snow avalanches. *In: Rockslides and avalanches* Vol **1**, 753-792, (Voight, B., ed.), Elsevier.

Murty, B.S. and Eswaran, V. 1994a
A shock-capturing scheme for avalanche modelling. *Extended abstracts, Int. symp. on snow and related manifestations, Snow & Avalanche Study Establishment, Manali (HP), India,* Sep. 1994.

Murty, B.S. and Eswaran, V. 1994b
Numerical Modelling of Avalanches. *Report submitted to Snow & Avalanche Study Establishment, Manali (HP), India,* May 1994.

Nohguchi, Y. 1989
Three-dimensional equations for mass centre motion of an avalanche of arbitrary configuration. *Annals of Glaciology* Vol. **13**, 215-217.

Nohguchi, Y., Hutter, K. and Savage, S.B. 1989
Similarity solutions for a finite mass granular avalanche with variable friction. *Continuum Mech. Thermodyn.* **1**, 239-265.

Computational models for dense snow avalanche motion

Report No: 581250-3
Date: 1996-04-30
Rev:
Rev. date:
Page: 44

NGI

Norem, H. 1992a
A general discussion on avalanche dynamics. *Norwegian Geotechnical Institute*, report **581200-25**.

Norem, H. 1992b
Simulation of snow-avalanche flow by a continuum granular model. *Norwegian Geotechnical Institute*, report **581200-26**.

Norem, H. 1995a
Shear stresses and boundary layers in snow avalanches. *Dr. Ing. Harald Norem A/S*, report **A951-1**.

Norem, H. 1995b
The Ryggfonn project, summary report 1981-1995. *Dr. Ing. Harald Norem A/S*, report **A952-1**.

Norem, H., Irgens, F. and Schieldrop, B. 1987
A continuum model for calculating snow avalanche velocities. *Proceedings of Avalanche Formation, Movements and Effects, Davos 1986,* IAHS publication **162**, 363-378.

Norem, H., Irgens, F. and Schieldrop, B. 1989
Simulation of Snow-Avalanche Flow in Run-Out Zones. *Annals of Glaciology* Vol. **13**, 218-225.

Norem, H., Locat, J. and Schieldrop, B. 1989
An approach to the physics and the modelling of submarine flowslides. *Norwegian Geotechnical Institute*, report **522090-2**.

Norem, H., Nishimura, K. and Maeno, N. 1992
Comparing model and full-scale experiments on snow avalanche dynamics. *Norwegian Geotechnical Institute*, report **581200-28**.

Norem, H. and Schieldrop, B. 1991
Stress analyses for numerical modelling of submarine flowslides. *Norwegian Geotechnical Institute*, report **522090-10**.

Perla, R.I. 1980
Avalanche Release, Motion and Impact. *Dynamics of Snow and Ice Masses,* Academic Press, Inc.

Perla, R.I., Cheng, T.T. and McClung, D.M. 1980
A Two-Parameter Model of Snow-Avalanche Motion. *Journal of Glaciology* Vol. **26**, No. **94**, 197-207.

Computational models for dense snow avalanche motion

Report No: 581250-3
Date: 1996-04-30
Rev:
Rev. date:
Page: 45

Salm, B. 1993
Flow, Flow Transition and Runout Distances of Flowing Avalanches. *Annals of Glaciology* Vol. **18**.

Salm, B., Burkard, A. og Gubler, H.U. 1990
Berechnung von Fließlawinen (Guideline for practitioners). Mitteilung nr. **47**, EISLF, Davos.

Savage, S.B. and Hutter, K. 1989
The motion of a finite mass of granular material down a rough incline. *J. Fluid Mech.* Vol. **199**, 177-215.

Savage, S.B. and Hutter, K. 1990
The dynamics of avalanches of granular materials from initiation to runout, Part I: Analysis. *Acta Mech.* **86**, 201-223 (1991).

Savage, S.B. and Nohguchi, Y. 1988
Similarity solutions for avalanches of granular materials down curved beds. *Acta Mech.* **75**, 153-174.

Scheiwiller, T. and Hutter, K. 1982
Lawinendynamik, Übersicht über Experimente und theoretische Modelle von Fließ- und Staublawinen. Mitteilung No. **58** der *Versuchsanstalt für Wasserbau, Hydrologie und Glaziologie an der Eidgenößischen Technischen Hochschule (Zürich),* 166 pp.

Takahashi, T. 1991
Debris flow. *International Association of Hydraulic Research.* A.A. Balkema, Rotterdam, The Netherlands.

Takahashi, T. and Yoshida, H. 1979
Study on the deposition of debris flows, Part I - Deposition due to abrupt change of bedslope. *Annals, Disaster Prevention Research Institute, Kyoto University, Japan,* **22 B-2** (In Japanese with English abstract).

Tesche, T.W. 1986
A three dimensional dynamic model of turbulent avalanche flow. *Proc. Int. Snow Science Workshop, Lake Tahoe California,* 1-27.

Voellmy, A. 1955
Über die Zerstörungskraft von Lawinen. *Schweiz. Bauzeitung* **73**, 159-165, 212-217, 246-249, 280-285.

Yoshimatsu, H. 1991
Study of the mechanics of debris flow and its simulation model. *Journal of Japan Landslide Society* **28-2**.

Computational models for dense snow avalanche motion

Report No: 581250-3
Date: 1996-04-30
Rev:
Rev. date:
Page: 46

NGI

Zenke, B. and Hildebrandt, M. 1983
Vorschlag eines statistisch-graphischen Verfahrens zur Lawinenreichweiten-bestimmung auf unstetigen Strichen, Wildbach- und Lawinenverbau. *Wildbach- und Lawinenverbau,* **47** Jg, Heft **2, Nov. 1983** (in German).

048. Bra-Trykk AS

Kontroll- og referanseside/
Review and reference document

NGI

Oppdragsgiver/*Client*	**Dokument nr/***Document No.* 581250-3
Kontraktsreferanse/ **Contract reference**	**Dato/***Date* 30 April 1996

Dokumenttittel/*Document title* Computational models for avalanche motion **Prosjektleder/***Project Manager* Karstein Lied **Utarbeidet av/***Prepared by* Carl B. Harbitz	**Distribusjon/***Distribution* ☐ **Fri/***Unlimited* ☒ **Begrenset/***Limited* ☐ **Ingen/***None*

Emneord/*Keywords*
Snow avalanche, runout distance, computation, dynamic motion

Land, fylke/*Country, County* **Kommune/***Municipality* **Sted/***Location* **Kartblad/***Map* **UTM-koordinater/***UTM-coordinates*	**Havområde/***Offshore area* **Feltnavn/***Field name* **Sted/***Location* **Felt, blokknr./***Field, Block No.*

Kvalitetssikring i henhold til/*Quality assurance according to*
NS-EN ISO9001

Kon- trollert av/ Reviewed by	Kontrolltype/ *Type of review*	Dokument/*Document*		Revisjon 1/*Revision 1*		Revisjon 2/*Revision 2*	
		Kontrollert/*Reviewed*		Kontrollert/*Reviewed*		Kontrollert/*Reviewed*	
		Dato/*Date*	Sign.	Dato/*Date*	Sign.	Dato/*Date*	Sign.
KL	Helhetsvurdering/ *General* *Evaluation* *	30/5	*(sign)*				
KL	Språk/*Style*	30/5	*(sign)*				
KL	Teknisk/*Technical* - Skjønn/*Intelligence* - Total/*Extensive* - Tverrfaglig/ *Interdisciplinary*						
KL	Utforming/*Layout*	30/5	*(sign)*				
CH	Slutt/*Final*	30/5-96	CH				
JGS	Kopiering/*Copy quality*	31/5-96	JS-				

* Gjennomlesning av hele rapporten og skjønnsmessig vurdering av innhold og presentasjonsform/
 On the basis of an overall evaluation of the report, its technical content and form of presentation

Dokumentet godkjent for utsendelse/ *Document approved for release*	**Dato/***Date* 30/5	**Sign.** *Carl B. Harbitz*